Catalysis Science & Technology

www.rsc.org/catalysis

Volume 1 | Number 1 | Jan 2013 | Pages 1–100

ROYAL SOCIETY OF CHEMISTRY

This is an *Accepted Manuscript*, which has been through the Royal Society of Chemistry peer review process and has been accepted for publication.

Accepted Manuscripts are published online shortly after acceptance, before technical editing, formatting and proof reading. Using this free service, authors can make their results available to the community, in citable form, before we publish the edited article. We will replace this *Accepted Manuscript* with the edited and formatted *Advance Article* as soon as it is available.

You can find more information about *Accepted Manuscripts* in the **Information for Authors**.

Please note that technical editing may introduce minor changes to the text and/or graphics, which may alter content. The journal's standard **Terms & Conditions** and the **Ethical guidelines** still apply. In no event shall the Royal Society of Chemistry be held responsible for any errors or omissions in this *Accepted Manuscript* or any consequences arising from the use of any information it contains.

ROYAL SOCIETY OF CHEMISTRY

www.rsc.org/catalysis

Catalytic Science & Technology

PAPER

Cyclohexane oxidation over AFI molecular sieves: Effects of Cr, Co incorporation and crystal size

Decheng Liu, Baoquan Zhang, Xiufeng Liu, Jian Li[*]

Heteroatoms substituted AFI molecular sieves with different size and morphologies were synthesized in hydrothermal conditions and characterized by X-ray diffraction (XRD), scanning electron microscopy (SEM), UV-vis diffuse reflectance spectroscopy (UV-vis), Fourier transform infrared spectroscopy (FT-IR), N_2 adsorption/desorption isotherm, inductively coupled plasma-optical emission spectrometry (ICP-
10 OES) and thermogravimetric analysis(TG-DTG). Uniformly sized plate-like crystals as thin as 400 nm were prepared using seed inducing method. Cr and Co ions were introduced into the molecular sieves and part of them was transformed to the high-valence state through calcination. In the reaction of cyclohexane oxidation, bimetal substituted $AlPO_4$-5 exhibited higher catalytic activities than single metal substituted analogues though the doping amount is lower. The improvement of diffusion efficiency resulting from the
15 shortening of the channels along the c-axis increased the conversion of cyclohexane significantly.

1. Introduction

After the first successful synthesis of aluminophosphate molecular sieves (APOs) in 1982,[1] the silicon and metals
20 substituted aluminophosphates were prepared with a variety of structure types and framework compositions.[2,3] The replacement of framework aluminum and phosphorus by silicon and metals can create acidic and redox sites, which are active centers for catalytic reactions. Among them, the AFI-type molecular sieves, consisting of straight channels with pore diameter of 7.3 Å, have
25 drawn considerable attentions in the catalytic field. There have been numerous reports focusing on the synthesis of heteroatoms substituted AFI molecular sieves and their catalytic performances, including TAPO-5 materials for the oxidation of cyclohexene,[4] metal-AFI for the alkylation of biphenyl,[5] FeAlPO-
30 5 for selective oxidation of benzene to phenol,[6] and MgAPO-5 molecular sieves for n-hexane cracking.[7]

One of the most researched areas of APOs in catalysis is the oxidation of linear and cyclic hydrocarbons.[8,9] Metal-doped AFI molecular sieves have shown potential as catalysts in the
35 selective oxidation of cyclohexane, which is a significant process in the synthetic fiber industry for the manufacture of Nylon-6 and Nylon-6,6.[10] In fact, molecular oxygen or air is used as the oxidant mainly due to the relatively low cost with limited waste problems.[11-21] However, the reaction in liquid phase using
40 molecular oxygen is a radical chain process, during which the intermediate alkylperoxy and alkoxy radicals are largely indiscriminate in their reactivity.[22] Raja et al obtained encouraging results in the oxidation of cyclohexene using another eco-friendly oxidant H_2O_2 as the oxidant and microporous

45 FeAlPO-5 as catalyst under moderate temperature. To achieve the same conversion using air as the oxidant, however, still faces challenges.[23] In addition, the oxidation using O_2 usually needs a high pressure reaction system while the simplicity of operation using H_2O_2 makes the total cost of equipment and raw materials
50 comparable or even lower than the oxidation employing O_2.

AFI molecular sieves doped with heteroatoms were already tested in the cyclohexane oxidation in the presence of H_2O_2.[24,25] However, it is still a challenge to achieve high efficiency in this reaction though many attempts have been made in liquid phase
55 using heterogeneous catalyst.[26] It was reported that AFI molecular sieves incorporated with three metals simultaneously showed higher activity than mono-substituted analogues in the cyclohexane oxidation with molecular oxygen.[21] Simultaneously framework incorporation of heavy metals into aluminophosphates
60 framework generates bimetallic active sites, which exhibit high activity and selectivity in the catalytic oxidations through synergistic interactions.[27] The effect of SAPO-34 crystallite size on the catalytic activity and lifetime in the methanol-to-olefins reaction was investigated, revealing a significant change of
65 diffusion limitation due to the transport resistance.[28,29] Hierarchical CrAPO-5, with lower diffusion resistance, exhibit higher catalytic activity and stability than microporous analogues.[30] The type and number of active sites, as well as the length of the diffusion path, would be of great importance in the
70 catalyst performances.

In this work, AFI molecular sieves incorporated with single or double metals were synthesized. Crystals with different size were prepared controllably through in-situ or seed inducing methods. The influence of bimetallic active sites and diffusion path on the

catalytic performance of AFI molecular sieves in the cyclohexane oxidation in relatively mild conditions was investigated. The coordination environment and the oxidation state of the transition metals and the stability of the catalysts were discussed in detail.

5 ## 2. Experimental

2.1 Catalyst preparation

AFI molecular sieves were hydrothermally synthesized. Cr and Co salts were added separately or together to provide active sites and manipulate the morphology of crystals. Aluminum 10 isopropoxide (AIP, 99.5%, Aldrich) was first hydrolyzed in DI water at the temperature of 80 °C using a water bath heating under stirring for 12 h to form a translucent alumina sol. After cooling down naturally, orthophosphoric acid (H_3PO_4, 85%, Tianjin Chemical Reagent Co., Inc) was dropped into the alumina 15 sol under stirring at 25 °C. Then, the solution was stirred for 10 h to form a white uniform gelation. Afterwards, triethylamine (TEA, 99%, Tianjin Chemical Reagent Co., Inc) was added sequentially under vigorous stirring, followed by stirring for 2 h and aging at room temperature for 10 h. The final molar ratio of the synthesis 20 solution was Al_2O_3 : $1.3P_2O_5$: 2.4TEA : $200H_2O$ (: $0.0125Cr_2O_3$: 0.025CoO). Aqueous solution of metal salts ($Cr(NO_3)_3 \cdot 9H_2O$ or $Co(CH_3COO)_2 \cdot 4H_2O$) was added into the synthetic solution alone or together, with the molar ratio of Cr_2O_3/Al_2O_3 = 0.0125, CoO/Al_2O_3 = 0.025. The precursor gel (30 mL) was loaded into a 25 50 mL Teflon-lined autoclave, which was then sealed and placed the oven. After crystallization at 180 °C for 72 h, the as-synthesized materials were recovered by centrifugation and thoroughly washed with deionized water several times followed by drying at 110 °C overnight.

30 Plate-like CrCoAPO-5 with smaller crystal size and lower aspect ratio, denoted as CrCoAPO-5 (sc), was synthesized using seed inducing method according to the procedure exploited by our group.[30] In the seed inducing synthesis, the aqueous suspension of seed (1 wt%) was prepared through stirring and 35 ultrasonic treatment repeatedly. After the synthesis solution was prepared with the same procedure as above mentioned at a temperature of 5 °C, 0.2 mL of seed suspension was added into the synthetic solution before aging. The precursor gel was crystallized at 150 °C for 5 h followed by cooling to room 40 temperature and being washed thoroughly and dried.

For comparison, 1.0 g $AlPO_4$-5 particles was impregnated with 100 mL aqueous solution containing 1 mmol $Cr(NO3)3 \cdot 9H2O$ at 90 °C in oil bath for 24 h. This sample, designated as Cr/APO-5, was separated by centrifugation, washed and dried. All of the 45 solid powders were calcined at 550 °C for 6 h in tube furnace to remove the template completely before use.

2.2 Catalyst characterization and leaching test

X-ray diffraction (XRD) data were obtained on a Rigaku D-max2500v/pc X-ray diffractometer using Cu Kα radiation (λ 50 =1.5418 Å) scanning in the range of 2θ = 5~50° at a scanning rate of 4 °/min. Scanning electron microscopy (SEM) was performed using a FEI Nanosem 430 field emission scanning electron microscopy (FE-SEM) at an acceleration voltage of 10~20 kV. UV-vis diffuse reflectance spectra were recorded by using a 55 Thermo Evolution 300 BB spectrophotometer, equipped with an integrated sphere. The amount of metal elements in the molecular

sieves was analyzed by a Varian Vista MPX inductively coupled plasma-optical emission spectrometry (ICP-OES). Thermogravimetric analysis was conducted using a TA-Q5000 60 instrument with a heating rate of 10 °C/min. FT-IR spectra was obtained for a resolution of 4 cm^{-1} at room temperature using KBr media using Thermo Scientific Nicolet 6700 Fourier transform infrared spectrometer. Nitrogen adsorption-desorption isotherms were measured at 77 K on a Micrometritics ASAP 2020 65 automatic surface area analyzer. Samples were degassed at 250 °C for 6 h prior to the measurements.

2.3 Catalytic performances and leaching test

The reaction of cyclohexane oxidation was carried out at 90 °C in a 50 mL Teflon-lined stainless steel autoclave under stirring in 70 oil bath for a given duration. A typical batch is as follows: 18.5 mmol of cyclohexane (99.5%, Tianjin Taixing Chemical Co., Ltd), 2.10 g of H_2O_2 aqueous solution (30%, Tianjin Guangfu Fine Chemical Research Institute), 0.1 g of catalyst and 10 mL acetone (99.5%, Tianjin Jiangtian Chemical Technology Co., 75 Ltd). After the reaction, the catalyst was separated through centrifugation, washed with acetone and reused again. The content of residual H_2O_2 was determined by the classical potassium permanganate titration method. The product was analyzed with a Agilent 6890 Gas Chromatograph equipped with 80 an HP-Innowax column (60 m × 0.32 mm) and a flame ionization detector using isobutanol as internal standard.

The leaching test was carried out by separating the catalyst from the reaction mixture after 10 h reaction. The amount of Cr leaching from the molecular sieves under the reaction condition 85 conditions was determined with spectrophotometric method using diphenyl carbazide as an indicator (measured at 545 nm). The leaching Co was determined using a fading spectrophotometry in the potassium thiocyanate-light green system with the maximum fading wavelength at 624 nm. The filtrate mixture was sealed 90 again for an additional period of further reaction at 90 °C.

3. Results and discussion

3.1 Physico-chemical characterization of AFI molecular sieves

Incorporation of heteroatoms could manipulate the morphology of crystals and introduce active sites such as acid sites or redox 95 sites. The SEM images of AFI crystals as shown in Fig. 1 indicated that most of the crystals exhibited hexagonal prismatic morphologies except CoAPO-5, which were mainly spherical aggregates. The incorporation of heteroatoms shortened the length of the crystallographic c-axis obviously. In comparison 100 with the crystals synthesized by traditional heating method, the AFI molecular sieves prepared using seed-inducing method exhibit much uniformly smaller particle size (2-4 μm) and lower aspect ratio (lower than 0.2). Therefore, the channel length along the c-axis of the AFI molecular sieves decreased from 20 μm to 105 less than 400 nm.

In XRD patterns as shown in Fig. 2, all the diffraction peaks can be attributed to the AFI structure, demonstrating that the crystallization products are highly crystallized AFI molecular sieves. The enhancement of (100) diffraction peak and decrease 110 of (002) diffraction peak of $AlPO_4$-5 suggest that the crystals aligned mainly with their c-axis parallel to the bottom plane, in accordance with the rod-like morphology in the SEM image.
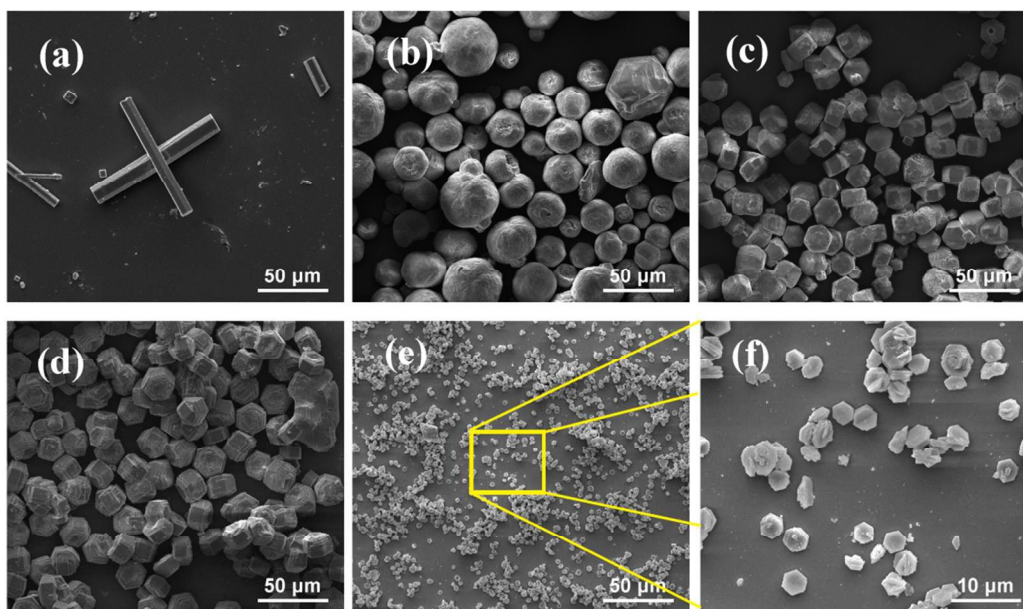
Fig. 1 SEM images of as-synthesized non-substituted and heteroatom-substituted AFI molecular sieves. (a) $AlPO_4$-5, (b) CoAPO-5,

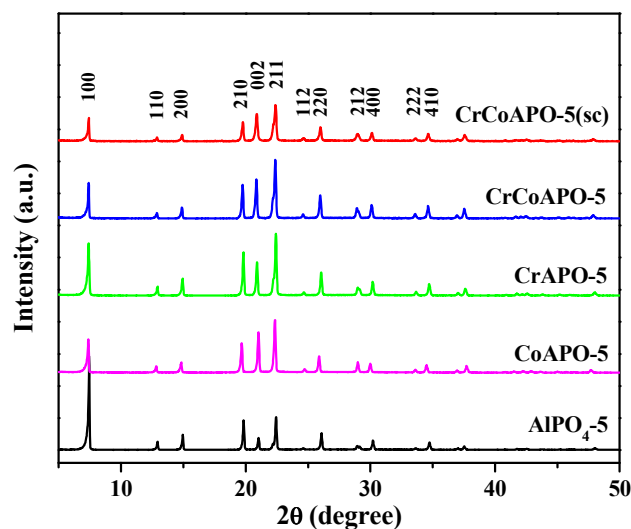(c) CrAPO-5, (d) CrCoAPO-5, (e,f) CrCoAPO-5(sc).

Fig. 2 XRD patterns of as-synthesized non-substituted and heteroatom-substituted AFI molecular sieves.

Fig. 3 shows the UV-vis spectra of the as-synthesized Cr/APO-5, CrAPO-5, CoAPO-5 and CrCoAPO-5 powders. The absorption bands of Cr/APO-5 appearing at 440 and 620 nm are generally recognized as the feature of Cr^{3+} in distorted octahedral coordination, but the absorbance was much lower than CrAPO-5, implying the lower content of octahedrally coordinated Cr in Cr/APO-5. However, the Cr content in Cr/APO-5 as shown in Table 1 is higher than that in CrAPO-5. This phenomenon is in accordance with that reported by Gläser and Laha, indicating that the Cr species introduced through impregnation are not only present as octahedrally coordinated chromium^{3+}, but as several multivalent CrO_x species.[32] The triplet bands in the range of 530-650 nm in the spectrum of CoAPO-5 can be attributed to d-d

transitions of tetrahedrally coordinated Co^{2+} ions.[31, 32] In CrCoAPO-5 molecular sieves, the peak of Cr^{3+} at 440 nm is still obvious, while the adsorption band at 620 nm is covered by the triplet bands of Co^{2+}, this result is in accordance with the spectrum of reported in reference.[24] In addition, the UV-vis spectrum of CrCoAPO-5(sc) is nearly the same as that of CrCoAPO-5 crystals except that the absorbance of the former was a little lower (data not shown).

There is still a controversy about the framework substitution of Chromium into the $AlPO_4$-5 crystals. Kornatowski et al reported that Cr heteroatoms are 4-fold bonded to the framework and complementarily coordinated by two additional ligands from the pores to give the distorted octahedral coordination, as evidenced by the violet color during calcination.[33] Kevan et al used electron spin echo modulation (ESEM) to demonstrate that Cr^{5+} substitute for phosphorus in a framework site in calcined CrAPSO-5.[34] However, Weckhuysen and Schoonheydt claimed that Cr^{3+} was not incorporated into the framework, but was present at the surface of the $AlPO_4$-5 crystals as octahedral ions which was partially oxidized by calcination to chromate and Cr^{5+}.[35] Despite of this, the consensus among all of the researchers is that the absorption peaks at 440 and 620 nm come from octahedrally coordinated Cr^{3+}, and the band at 360 nm is the features of charge transfer from O to Cr^{6+} ions. Therefore, the existence of the Cr^{3+} and Cr^{6+} containing species in these molecular sieves was in no doubt.

In the UV-vis spectra of the calcined molecular sieves as shown in Fig. 4, the d-d bands of Cr/APO-5 were largely weakened owing to the oxidation from Cr^{3+} to Cr^{6+}, which was characterized by the high intensity O→Cr charge transfer band at 360 nm,[36] suggesting most of the Cr^{3+} species were oxidized to the Cr^{6+} state. While in the spectrum of calcined CrAPO-5, the bands at 290, 440 and 620 nm still exhibit relatively high
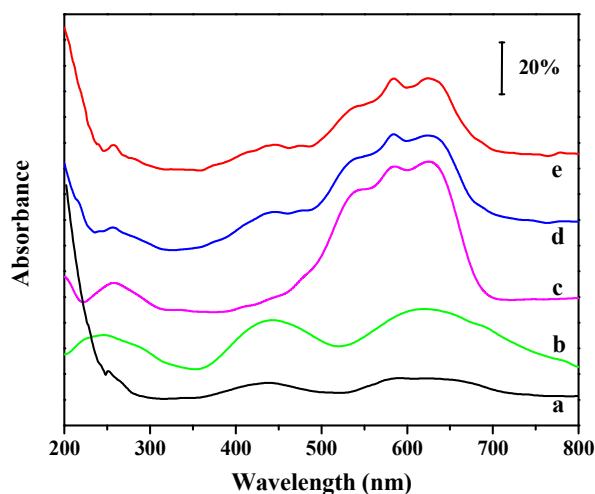
Fig. 3 UV-vis spectra of as-synthesized (a) Cr/APO-5, (b) CrAPO-5, (c)CoAPO-5, (d) CrCoAPO-5 and (e) CrCoAPO-5(sc) molecular sieves.
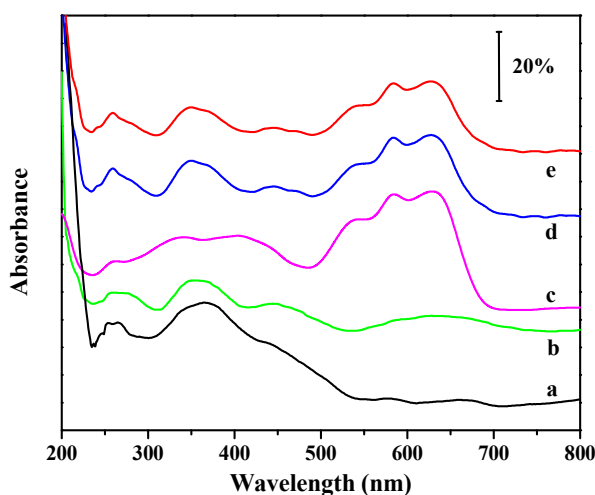

Fig. 4 UV-vis spectra of calcined (a) Cr/APO-5, (b) CrAPO-5, (c)CoAPO-5, (d) CrCoAPO-5 and (e) CrCoAPO-5(sc) molecular sieves.

intensity, demonstrating that only part of the Cr^{3+} was oxidized to the high state. In addition, there were probably the same Cr-containing species in both of them. The intensity of triplet bands in the spectra of CoAPO-5 was reduced, whilst two intense bands appeared centered at 340 and 400 nm can be attributed to tetrahedrally cooperated Co^{3+}. The new peaks in the spectrum of CrCoAPO-5 after calcination suggest that both of the transition metals coexist in a variety of valence after calcination though some peaks were covered by other stronger ones (Fig. 4d and e). Therefore, the molecular sieves containing metals with multiple valence states have potential in catalytic oxidation reactions.

The relative molar composition of AFI crystals and the synthetic solution were listed in Table 1. In single metal doped molecular sieves, the doping amount of heteroatoms is more than the bimetal incorporated analogues, which was in accordance with the UV-vis spectra (Fig. 3). The Cr and Co contents in the CrCoAPO-5 molecular sieves were similar as that in the synthetic solution, where Co seemed to incorporate into the molecular sieves a little more easily. These results and UV-vis spectra revealed that Co and Cr were incorporated into the AFI molecular sieves, however, the doping amount of heteroatoms in CrCoAPO-5(sc) was slightly less than the larger crystals.

Table 1 Elemental molar composition of AFI molecular sieves analysis by ICP-OES

Samples	Synthetic solution			AFI crystals		
	P	Co	Cr	P	Co	Cr
CoAPO-5	1	0.0096	-	1	0.0131	-
CrAPO-5	1	-	0.0096	1	-	0.0159
Cr/APO-5 [a]	1	-	-	1	-	0.0212
CrCoAPO-5	1	0.0096	0.0096	1	0.0125	0.0091
CrCoAPO-5 (sc)	1	0.0096	0.0096	1	0.0104	0.0078

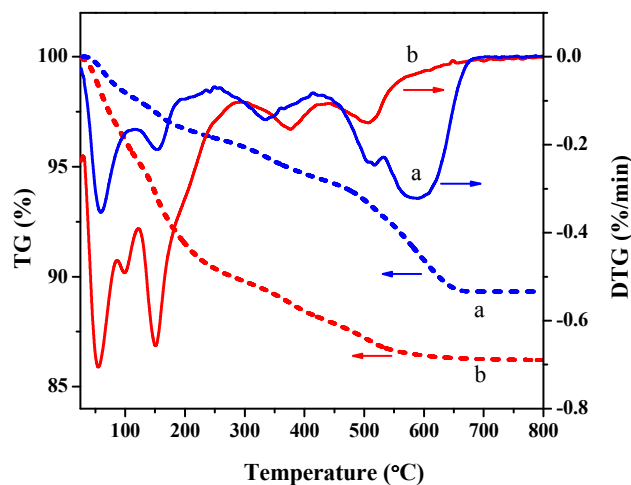[a]: impregnated with aqueous solution containing 1 mmol $Cr(NO_3)_3 \cdot 9H_2O$

Fig. 5 TG-DTG curves of the as-synthesized (a) CrCoAPO-5 and (b)CrCoAPO-5(sc).

The TG-DTG profiles and the mass loss at different stages of CrCoAPO-5 with different crystal sizes were shown in Fig. 5 and Table 2, the first two stages could be attributed to the physical desorption of water and the template (TEA) on the surface and in the pore systems, respectively. With larger external surface, the CrCoAPO-5(sc) adsorbed more water than CrCoAPO-5, resulting in the different total mass loss. Water and TEA molecules could diffuse out of the crystal more easily due to the shorter channels of smaller particles. Therefore, the mass loss at low temperature region was much more in CrCoAPO-5(sc). The mass loss at 260-420 °C came from the decomposition of the template. In CrCoAPO-5 with larger crystal size, a large proportion of TEA was transformed into complex compounds before transporting out of the channels, which need to be calcined in much higher temperature. In the range of 420-700 °C, the complex oxidation product was decomposed completely. The different proportion of mass loss in the high temperature suggested that molecular sieves with smaller particle size provided decreased diffusion barrier for molecules to diffuse.

In the FT-IR spectra of the as-synthesized molecular sieves as shown in Fig.6, the vibration bands of the AFI framework at 1118 and 479 cm^{-1} for $AlPO_4$-5, were shifted to 1104 and 468 cm^{-1} for CrCoAPO-5, providing a possible hint for the incorporation of metals into the framework because of the longer bonds of Co-O and Cr-O than Al-O.[37] The absorption bands in the range of 2850-2960 cm^{-1} come from the stretching vibration of C-H bonds of -CH_3, the bands near 2750 cm^{-1} are assigned to the C-H bonds in -CH_2-N, the peaks at 1475 cm^{-1} and 740 cm^{-1} can be attributed to bending vibration and in-plane rocking vibration of C-H bonds, respectively. The peak near 1240 cm^{-1} comes from the stretching

Table 2 TG data of CrCoAPO-5 in air atmosphere

Temperature Range (°C)	CrCoAPO-5		CrCoAPO-5(sc)	
	Mass Loss (%)	Total Mass Loss (%)	Mass Loss (%)	Total Mass Loss (%)
I.30~120	1.94	1.94	4.78	4.78
II.120~260	1.77	3.71	5.37	10.15
III.260~420	1.77	5.48	1.88	12.03
IV.420~700	5.21	10.69	1.76	13.79

Table 3 Texture properties of AFI molecular sieves calculated from nitrogen physisorption data

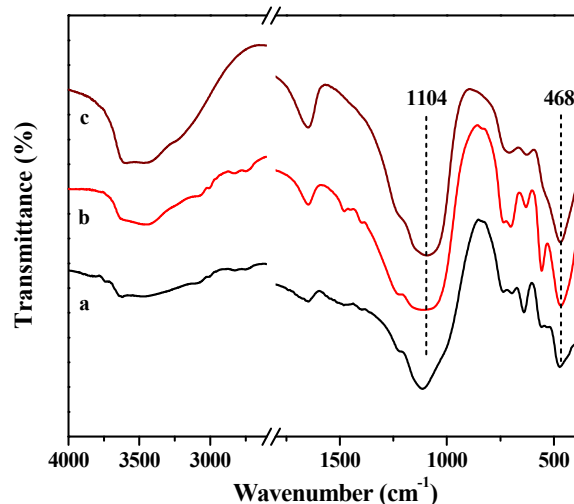| Samples	S_{BET} (m²/g)	$S_{External}$ (m²/g)	V_{Pore} (cm³/g)[a]
CoAPO-5	244	39	0.110
CrAPO-5	279	51	0.119
Cr/APO-5	42	26	0.023
CrCoAPO-5	266	15	0.131
CrCoAPO-5 (sc)	265	24	0.126

[a] Calculated by the t-plot method.

Fig. 6 FT-IR spectra of the as-synthesized AlPO$_4$-5(a), as-synthesized CrCoAPO-5 (b) and calcined CrCoAPO-5(c).

vibration of C-N bonds. All of the above absorption bands coming from the template disappeared after calcination, which demonstrated the complete removal of the template, allowing the active sites accessible to the reactant molecules.

The specific surface area and pore volumes of calcined samples calculated using the isothermal data were listed in Table 3. in which the AFI molecular sieves doped with metals directly in the synthesis process had S_{BET} and V_{pore} in good agreement with literature report, revealed that the channels of molecular sieves were opened up for the reactant molecules to diffuse. The catalyst prepared by wet-impregnation showed a dramatic decrease in the specific surface area especially the internal surface area, despite the lower loadings of Cr than their in situ synthesized counterpart. These data indicated that even if the Cr species in the CrAPO-5 and CrCoAPO-5 exist as extra-framework aggregates, they would be highly dispersed and consequently did not block the AFI micropores. The decrease of the external surface area of CrCoAPO-5 molecular sieves may come from the smoothness of the crystal surfaces.

3.2 Catalytic performance

The calcined samples were used as catalysts in the oxidation of cyclohexane and the results were summarized in Table 4. Theoretically, the AlPO$_4$-5 molecular sieves exhibit no catalytic activity due to the neutral framework. The slight conversion increase using AlPO$_4$-5 compared with blank experiment may result from defects in crystals. Incorporation of Co or Cr into the AFI molecular sieves increased their catalytic activity obviously, where the effect of Cr was more pronounced. The Cr/APO-5 catalyst showed activity higher than AlPO$_4$-5 but lower than CrAPO-5. This observation can be explained as that Cr species in

the AFI molecular sieves played a catalytic role but the micropores was blocked limiting the access of the reactant to the active sites.

Simultaneous incorporation of Cr and Co into molecular sieves generated novel bimetallic active sites, which provided increase of selectivity and activity in the catalytic oxidations, compared to analogues mono-metallic systems. In the study of Xu's group on the catalytic properties of FeCoMnAPO-5 for the liquid phase oxidation of cyclohexane,[38] a possible explanation about the synergistic effect was proposed that the reaction was mainly initiated by cobalt sites, then the intermediate product cyclohexyl hydroperoxide migrated to adjacent manganese sites to decompose to ketone and alcohol, and the alcohol was further oxidized to ketone over the iron site. But it is worth to confirm whether the individual metal sites perform only one of these roles considering the fact that single metal substituted AlPO$_4$-5 still showed catalytic activity to a certain extent. Raja's group precisely controlled the local environment, redox behavior, and coordination geometry of the bimetallic species in the VTiAPO-5 catalyst to investigate the role of each active site in the catalytic process.[39] Through the formation of peroxo species, the oxophilic titanium center is more likely to bind to the oxidant and activate it. Then the vanadium ions, with a lower redox barrier, will catalyze the reaction more efficiently once a proximal titanium center has activated the oxidant. The ability to facilitate catalytic synergy relied not only the position and distribution of the individual metal ions within the framework, but the proximity of the two metals could play a pivotal role in enhancing the catalytic activity. The detailed information about the exact nature of the active sites and their synergistic effect is under investigation to acquire the structure-property correlations.

As demonstrated via TG-DTG techniques, smaller particle size means a decrease of diffusion path length for reactant and product molecules to diffuse in and out of the molecular sieves. Therefore the catalysis efficiency would be enhanced significantly. The conversion of cyclohexane was increased by 130% on the catalysis of CrCoAPO-5(sc). Though the content of metals is only one quarter of that reported in reference,[24, 40] the conversion of CrCoAPO-5(sc) was nearly the same as the most active catalyst in half the reaction time(Table 5). In addition, the leaching of metals was largely suppressed probably due to the shorter contact time between polar molecules and metal sites. It is worth to note that the 50% conversion in reference 40 using acetic acid as solvent may be questionable because the AFI crystals would be resolved in acidic conditions. The author also claimed that the lifetime of the catalyst in acetic acid was decreased obviously. Furthermore, our reaction products contained only cyclohexanol and cyclohexanone without detectable by-product. The high K/A oil selectivity is advantageous for the industrial application.

Table 4 Catalytic performances of different heteroatom substituted AFI molecular sieves for the oxidation of cyclohexane

Sample	Crystal size (μm)	Conversion (%)	Selectivity (%)		
			Cyclohexanol	Cyclohexanone	Others
none	-	0.4-0.8	46.8	45.8	7.4
AlPO₄-5	30-40	0.7-1.0	43.7	47.5	8.8
CoAPO-5	20-40	2.54	42.0	58.0	-
CrAPO-5	20-25	3.78	46.0	54.0	-
Cr/APO-5	30-40	2.04	46.6	53.4	
CrCoAPO-5	25-30	6.85	43.7	56.3	-
CrCoAPO-5(sc)	2-4	15.97	44.8	55.2	-

Reaction conditions: catalyst 0.10 g, cyclohexane 18.5 mmol, acetone 10 mL, H_2O_2 18.5 mmol, T = 90 °C, t = 20 h.

Table 5 Comparison of catalytic performance of CrCoAPO-5 molecular sieves in liquid oxidation of cyclohexane with literatures

Oxidant	Temperature (°C)	Solvent	Time(h)	Conversion (%)	Doping amount		Leaching of Metals	Literature
					Co/Al	Cr/Al		
O_2(1MPa)	115	None	6	5.9	0.05	0.05	slightly	40
O_2(1MPa)	115	Cyclohexanol	6	4.2	0.05	0.05	mildly	40
O_2(1MPa)	115	Acetic acid	6	50	0.05	0.05	mildly	40
H_2O_2	60	Acetone	40	3.9	0.05	0.05	seriously	24
H_2O_2	90	Acetone	10	~11	0.05	0.05	seriously	24
H_2O_2	90	Acetone	40	~17	0.05	0.05	seriously	24
H_2O_2	90	Acetone	20	15.97	0.0125	0.0125	mildly	This work

It is of great importance to make sure whether or not the reaction took place inside the micropores, because the increase in the catalytic activity could also be explained by the increase in external surface of the catalyst. Sheldon et al used CrAPO-5 as a heterogeneous catalyst for the liquid phase oxidation of olefins with tert-butyl hydroperoxide (TBHP) to the corresponding α,β-unsaturated ketones.[41] When the bulkier pinane hydroperoxide was used as the oxidant, reaction rate decreased dramatically, suggesting the reaction took place inside the micropores. In another report, the same group observed that the bulky triphenylmethyl hydroperoxide was hardly decomposed under the catalysis of CrAPO-5,[42] providing another evidence for the occurrence of the reaction in the micropores. In this work, the single metal substituted AFI molecular sieves own much higher external surface but lower catalytic activity, suggesting the contribution of the external surface would be rather limited. Though the external surface of CrCoAPO-5(sc) is 60% larger than CrCoAPO-5, the conversion over the former catalyst is 130% higher than the latter. Therefore even if the external surface contributed to the reaction to a certain degree, the active sites in the micropores still play the major role in this reaction.

3.3 The stability of the catalyst

In the filtration experiment, the catalyst was separated from the reaction mixture after 10 h, and the filtrate mixture was sealed again for an additional period of further reaction at 90 °C. The conversion of cyclohexane increased from 10.4% to 11.5% in the following 20 h (Fig. 7), which appeared to be mainly attributable to the homogeneous catalysis of leached Cr species (discussed below). However, the minor contribution from the reaction intermediates residual in the filtrate could not be ruled out. Whichever the reason, the homogeneous catalysis was rather limited, demonstrating that the major mechanism of the reaction was heterogeneous.
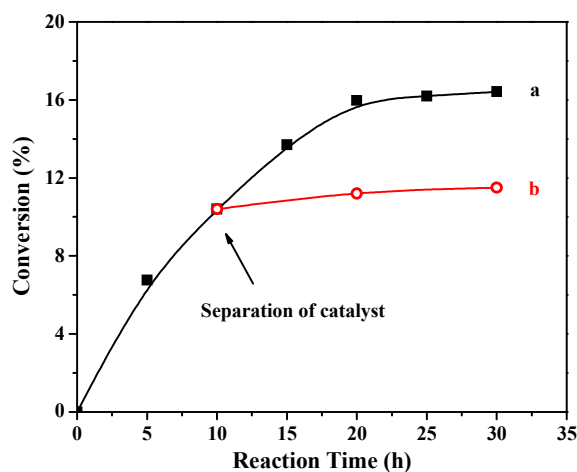

Fig. 7 Cyclohexane oxidation using H_2O_2 at 90 °C: (a) with CrCoAPO-5(sc) as the catalyst, (b) filtrate(catalyst separation after 10 h reaction).
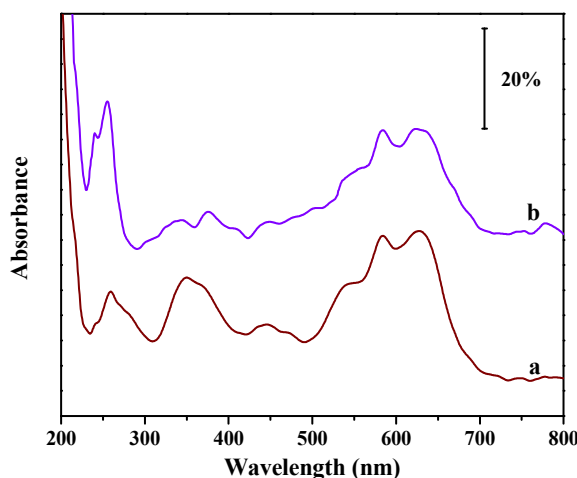

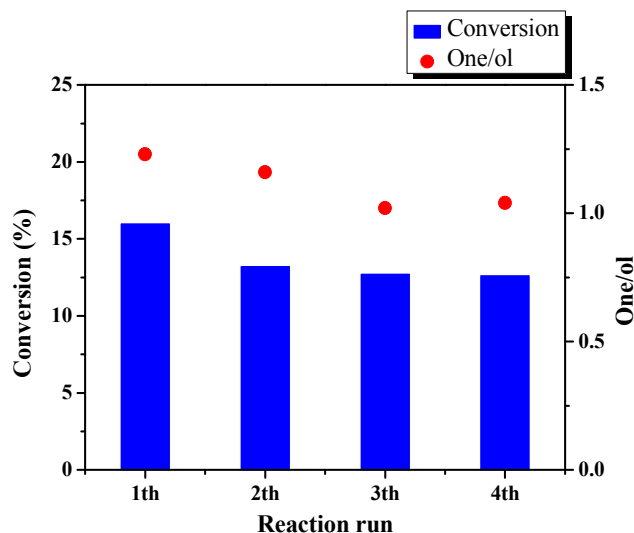**Fig. 8** UV-vis spectra of CrCoAPO-5(sc) (a) before and (b) after reaction.

Fig. 9 Recycling experiment of cyclohexane oxidation over CrCoAPO-5(sc) using H_2O_2 as the oxidant, T = 90 °C, t = 20 h.

The UV-vis spectra of recovered CrCoAPO-5(sc) (Fig. 8b) showed a weaker absorption peak at 360 nm than the new catalyst, suggesting some leaching of Cr ions, while the absorbance of tetrahedrally cooperated Co^{2+} and Co^{3+} went down only a little. According to the spectrophotometrical result, the amount of Cr and Co leaching from the catalyst was about 6% and 0.3%, respectively, consistent with the UV-vis spectra. Compared with Cr, the Co was harder to leach from the molecular sieves, suggesting it was tightly fixed in the framework.

When the catalyst was recovered after the 20 h reaction and reused again, the conversion of cyclohexane decreased to 13.2%, in accordance with the UV-vis spectra and leaching test. However, the decrease of reactivity coming from metal leaching seemed to stop when the CrCoAPO-5(sc) was reused several times (Fig 9). There are probably at least two kinds of Cr species in the CrCoAPO-5 catalyst. One connected with framework via weak forces, which was leached by polar molecules with ease. The other interacted with framework strongly, or even located in the framework position, making them hard to leach. Considering the leaching of Cr, the decrease of cyclohexanone/cyclohexanol ratio may be a proof that Cr ions promote the conversion from to alcohol the corresponding ketone.[43] In reference 24, the cyclohexanone/cyclohexanol ratio was kept above 3.0 using the catalyst with high Cr content, which would be another hint. This observation will be useful for further investigation of exact nature of the active sites and their synergistic effect.

4. Conclusions

Cr, Co and Cr-Co doped AFI molecular sieves were synthesized under hydrothermal conditions, showing different morphologies and crystal size. Slice-like crystals with small size and uniform morphology can be synthesized through seed inducing method. Several characterization techniques demonstrated that tetrahedrally coordinated Co^{2+} and octahedrally coordinated Cr^{3+} were introduced into the $AlPO_4$-5 and the calcination treatment oxidized part of them. The increased activity of the Cr-Co doped AFI molecular sieves in the cyclohexane oxidation may result from the synergistic interaction of Cr and Co. The shorter diffusion paths are apparently advantageous for enhanced diffusion of the organic molecules as compared to the longer channels of large crystals. Therefore the use of plate-like CrCoAPO-5(sc) as thin as 400 nm further increased the conversion of cyclohexane. The result of the recycling experiment revealed that the catalyst exhibit relative stability to some extent though a small amount of metal would leach from the molecular sieves.

Notes and references

State Key Laboratory of Chemical Engineering, School of Chemical Engineering and Technology, Tianjin University, Tianjin 300072, China Tel: +86-22-27408785, E-mail address: jian.li@tju.edu.cn

Acknowledgements

References

1 S. T. Wilson, B. M. Lok, C. A. Messina, T. R. Cannan and E. M. Flanigen, *J. Am. Chem. Soc.*, 1982, **104**, 1146.

2 B. M. Lok, C. A. Messina, R. L. Patton, R. T. Gajek, T. R. Cannan and E. M. Flanigen, *J. Am. Chem. Soc.*, 1984, **106**, 6092.

3 E. M. Flanigen, B. M. Lok, R. L. Patton and S. T. Wilson, *Pure Appl. Chem.*, 1986, **58**, 1351.

4 A. Alfayate, C. Márquez-Álvarez, M. Grande-Casas, B. Bernardo-Maestro, M. Sánchez-Sánchez and J. Pérez-Pariente, *Catal. Today*, 2013, **213**, 211.

5 H. Maekawa, S. K. Saha, S. Mulla, S. B. Waghmode, K. Komura, Y. Kubota and Y. Sugi, *J. Mol. Catal. A: Chem.*, 2007, **263**, 238.

6 N. R. Shiju, S. Fiddy, O. Sonntag, M. Stockenhuber and G. Sankar, *Chem. Commun.*, 2006, 4955.

7 L. L. Feng, X. Y. Qi, J. Y. Li, Y. L. Zhu and L. Q. Zhu, *React. Kinet. Catal. Lett.*, 2009, **98**, 327.

8 J. M. Thomas, R. Raja, G. Sankar and R. G. Bell, *Nature*, 1999, **398**, 227.

9 A. K. Suresh, M. M. Sharma and T. Sridhar, *Ind. Eng. Chem. Res.*, 2000, **39**, 3958.

10 J. M. Thomas, R. Raja, G. Sankar and R. G. Bell, *Acc. Chem. Res.*, 2001, **34**, 191.

11 S. Lin and H. Weng, *Appl. Catal., A.*, 1993, **105**, 289.

12 S. Lin and H. Weng, *Appl. Catal., A.*, 1994, **118**, 21.

13 R. Raja, G. Sankar and J. M. Thomas, *J. Am. Chem. Soc.*, 1999, **121**, 11926.

14 M. Dugal, G. Sankar, R. Raja and J. M. Thomas, *Angew. Chem. Int. Ed.*, 2000, **39**, 2310.

15 A. F. Masters, J. K. Beattie and A. L. Roa, *Catal. Lett.*, 2001, **75**, 159.

16 P. Tian, Z. M. Liu, Z. B. Wu, L. Xu and Y. L. He, *Catal. Today*, 2004, **93-95**, 735.

17 J. D. Chen and R. A. Sheldon, *J. Catal.*, 1995, **153**, 1.

18 G. Sankar, R. Raja and J. Thomas, *Catal. Lett.*, 1998, **55**, 15.

19 D. L. Vanoppen, D. E. De Vos, M. J. Genet, P. G. Rouxhet and P. A. Jacobs, *Angew. Chem. Int. Ed.*, 1995, **34**, 560.

20 J. Li, X. Li, Y. Shi, D. Mao and G. Lu, *Catal. Lett.*, 2010, **137**, 180.

21 L. P. Zhou, J. Xu, H. Miao, X. Q. Li and F. Wang, *Catal. Lett.*, 2005, **99**, 231.

22 C. W. Jones, *Applications of hydrogen peroxide and derivatives*, Royal Society of Chemistry, Cambridge, 1999.

23 R. Raja, S. Lee, M. Sanchez-Sanchez, G. Sankar, K. D. Harris, B. F. Johnson and J. M. Thomas, *Top. Catal.*, 2002, **20**, 85.

24 M. H. Zahedi-Niaki, M. P. Kapoor and S. Kaliaguine, *J. Catal.*, 1998, **177**, 231.

25 W. B. Fan, B. B. Fan, M. G. Song, T. H. Chen, R. F. Li, T. Dou, T. Tatsumi and B. M. Weckhuysen, *Microporous Mesoporous Mater.*, 2006, **94**, 348.

26 U. Schuchardt, D. Cardoso, R. Sercheli, R. Pereira, R. S. Da Cruz, M. C. Guerreiro, D. Mandelli, E. V. Spinacé and E. L. Pires, *Appl. Catal., A.*, 2001, **211**, 1.

27 M. E. Potter, A. J. Paterson and R. Raja, *ACS Catalysis*, 2012, **2**, 2446.

28 I. M. Dahl, R. Wendelbo, A. Andersen, D. Akporiaye, H. Mostad and T. Fuglerud, *Microporous Mesoporous Mater.*, 1999, **29**, 159.

29 N. Nishiyama, M. Kawaguchi, Y. Hirota, D. Van Vu, Y. Egashira and K. Ueyama, *Appl. Catal., A.*, 2009, **362**, 193.

30 J. Kim, S. Bhattacharjee, K. E. Jeong, S. Y. Jeong, M. Choi, R. Ryoo and W. S. Ahn, *New J. Chem.*, 2010, **34**, 2971.

31 J. Yan, J. Li, B. Q. Zhang and X. F. Liu, *Chinese J. Inorg. Chem.*, 2015, **31**, 749.

32 R. Gläser and S. C. Laha, *Catal. Commun.*, 2007, **8**, 91.

33 G. N. Karanikolos, H. Garcia, A. Corma and M. Tsapatsis, *Microporous Mesoporous Mater.*, 2008, **115**, 11.

34 D. Grandjean, A. M. Beale, A. V. Petukhov and B. M. Weckhuysen, *J. Am. Chem. Soc.*, 2005, **127**, 14454.

35 J. Kornatowski, G. Zadrozna, M. Rozwadowski, B. Zibrowius, F. Marlow and J. A. Lercher, *Chem. Mater.*, 2001, **13**, 4447.

36 Z. Zhu and L. Kevan, *Phys. Chem. Chem. Phys.*, 1999, **1**, 199.

37 B. M. Weckhuysen and R. A. Schoonheydt, *Zeolites*, 1994, **14**, 360.

38 P. A. Barrett, G. Sankar, C. R. A. Catlow and J. M. Thomas, *J. Phys. Chem.*, 1996, **100**, 8977.

39 L. Zhou, J. Xu, C. Chen, F. Wang and X. Li, *J. Porous Mater.*, 2008, **15**, 7.

40 R. M. Leithall, V. N. Shetti, S. Maurelli, M. Chiesa, E. Gianotti and R. Raja, *J. Am. Chem. Soc.*, 2013, **135**, 2915.

41 H. E. B. Lempers and R. A. Sheldon, *Appl. Catal., A.*, 1996, **143**, 137.

42 J. D. Chen, H. Lempers and R. A. Sheldon, *Colloids Surf., A.*, 1995, **101**, 137.

43 J. Muzart, *Chem. Rev.*, 1992, **92**, 113.

Table of content
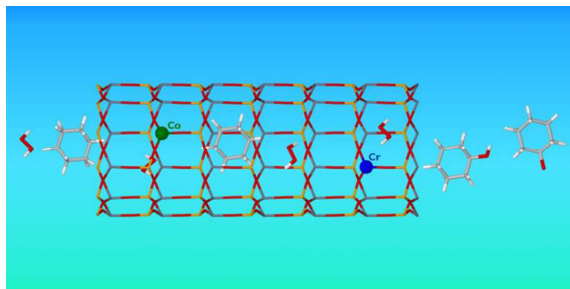
The ultra-thin AFI catalyst doped with Cr and Co exhibit enhanced activity in the oxidation of cyclohexane in mild conditions.